Hydrogen Production via Steam Reforming in a Reverse-Flow Reactor

Frank Hershkowitz, Paul J. Berlowitz, Richard F. Socha,
Elise Marucchi-Soos, Jeffrey W. Frederick

ExxonMobil Research and Engineering Company

As one begins to contemplate a broader use of hydrogen in our energy infrastructure, it is instructive to consider that our most economical route to hydrogen, Steam-Methane Reforming (SMR) is only 70-75% efficient to hydrogen. SMR inefficiency is rooted in a high-temperature endothermic nature of the reaction. Excess heat is lost in heating streams to reaction temperature and ineffectively using the sensible heat in product streams as they are returned to ambient conditions. Heat exchange can be added to improve efficiency, but the corrosive nature of the syngas makes this heat exchange costly and problematic.

Our approach to raising the efficiency of steam reforming is to perform this heat exchange within the catalyst bed itself. We operate the steam reforming bed as a reverse flow reactor, in which heat addition (by combustion) alternates with heat consumption (by reforming), with the flow being reversed between these steps. By properly designing the bed and other reactor components, the entire bed becomes a high-efficiency heat exchanger. With appropriate design, SMR efficiency can be boosted into the 85-90% range, within a few percent of the theoretical maximum.

We call this approach "Pressure Swing Reforming" (PSR) because we swing the pressure of the reactor such that low pressure air can be used during combustion, while high pressure syngas is produced as reform-product. In our previous publications (e.g. Hershkowitz, et. al. 2004) we have provided a general description of the process, some historical precedents from the literature, experimental results validating the concept, and some examples of how this new process might be used. These threads are not repeated. Here we present computer simulation results that illustrate some of the operating principles of an effective reverse-flow reactor system for methane-steam reforming.

Computer Simulation

The physics and chemistry of Pressure Swing Reforming have been programmed into a numerical simulation of the process. The model includes reforming kinetics (Xu and Froment for methane), heat transfer, pressure drop, axial conduction, and the relevant gas and solid properties. The computational approach is to divide the PSR bed into 30 cells, each representing $1/30^{th}$ of the bed, to treat each cell as a perfectly stirred reactor, and to march the simulation forward in time.

Increasing Space Velocity Only

The simulation results are summarized by graphing the end-of-regeneration and end-of-reforming step temperature profiles, as seen in Figure 1. In all simulations presented here the bed system is 30 cells long (numbered 2-31), and cells 2-12 are uncatalyzed. During the

regeneration step, fuel and air flow from cell 2 towards 31. Combustion reactions associated with cells 13-31 enable combustion to occur in those locations. During the reforming step, methane and steam flow from cell 31 towards 2. Reforming reactions associated with cells 13-31 enable reforming to occur in those locations. Refer to Hershkowitz (2004) for description of the transient behavior of the reactor system. Space velocity (C_1GHSV) is expressed as flow of reform feed carbon (as if C was a gas species) averaged over entire cycle and divided by total bed system volume. Such units enable productivity comparisons to other processes that may not be cyclic or which may have vastly different diluent requirements. The efficiency of the reaction cycle is expressed as the heat of combustion (ΔH_C) of product syngas divided by the ΔH_C of reactor fuel and feed.

Figure 1: End-of-step temperature profiles for 60ppi foam beds, 300°C inlet temperature and 15 second cycle time. Increasing space velocity shown in panels.

(a) 1000 C_1GHSV; 99.8% ΔH_C Recovery

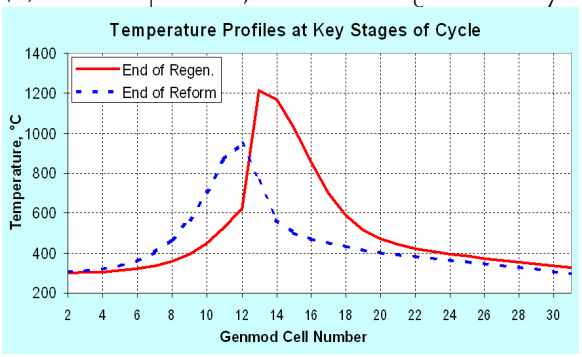

(b) 2000 C_1GHSV; 99.2% ΔH_C Recovery

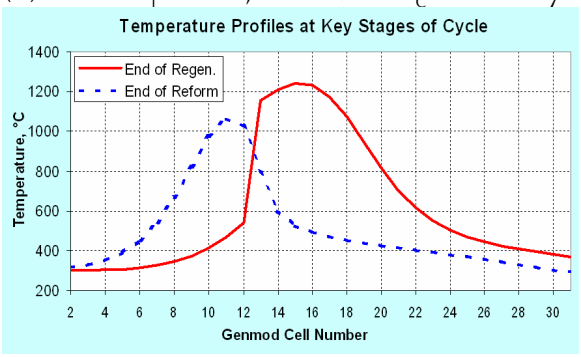

(c) 3000 C_1GHSV; 97.9% ΔH_C Recovery

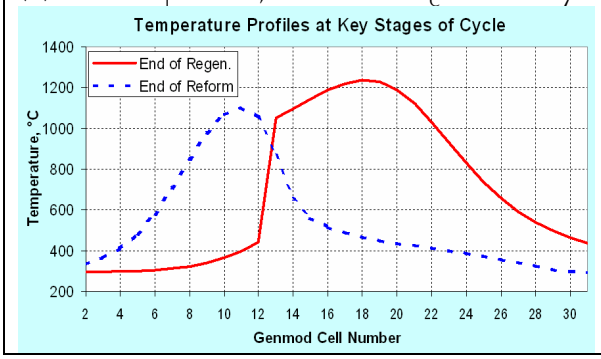

(d) 4000 C_1GHSV; 94.1% ΔH_C Recovery

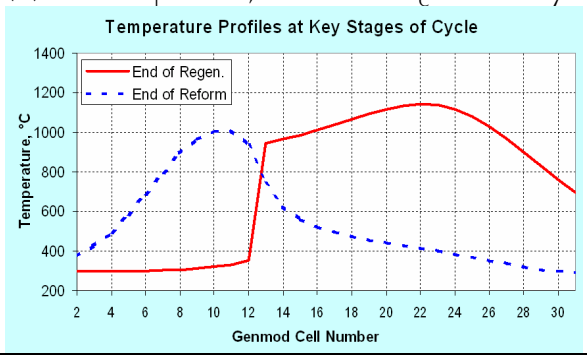

As space velocity increases at constant cycle time (τ_{cycle}), there is a proportional increase in the amount of heat that must be stored in the bed during the cycle to preserve conversion. This increase is observed in Figure 1 in the form of an increasing 'bubble' of heat within the bed system. The heat bubble begins at cell 13 where catalysis starts, and extends as far as needed to hold the required heat. When space velocity is low (1a), the high temperatures are far from the reactor ends. Consequently, products come out at temperatures very close to inlet temperatures. Under such conditions, these high temperature reactions are carried out essentially without heat loss, and heat value (ΔH_C) is conserved. As space velocity becomes so large that the bed can no longer contain the heat bubble (1d), products emerge from the bed with higher temperatures and some of the heat value (ΔH_C) of the feed is lost to heat in these product streams.

System Adjustments to Enable High Space Velocity

The space velocity limit described above is associated with the limited amount of heat that the bed can hold in a single reforming cycle. This limit can be overcome in two ways. Decreasing the cycle time, shown in Figure 2(a) reduces the amount of heat that must be held during the cycle, and thus shrinks the size of the heat bubble. A space velocity of 6000 is achieved in the 6 second cycle of 2(a), with a heat-bubble size slightly smaller than that of the 3000 C_1GHSV achieved with a 15 sec cycle in figure 1(c). Alternatively, the bed system can be adjusted to accommodate the higher heat storage that is required for high space velocity. This is illustrated in Figure 2(b), in which the packing is switched to a bead-bed packing that has a much higher heat capacity because of its relatively low void fraction (foam monoliths have void fractions of around 90%). The high heat capacity of the sphere bed enables 6000 space-velocity with a 15-second cycle, and does this with a smaller (in length, not enthalpy) heat bubble than could be accomplished at 2000 C_1GHSV using foam (Fig. 1b).

Figure 2: End-of-step temperature profiles for 300C inlet temperature. Achieving higher space velocity via reduced cycle time or higher bed heat capacity.

(a) 6 second cycle time & 60 ppi foam
6000 C_1GHSV; 97.4% ΔH_C Recovery

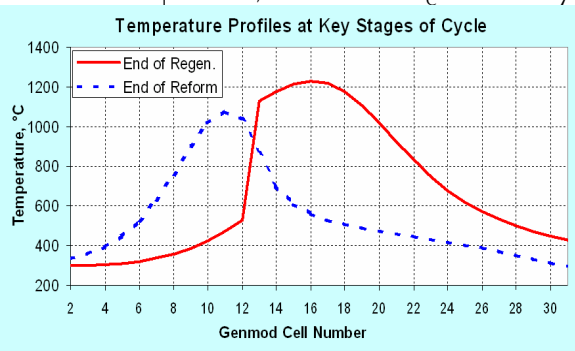

(b) 15 second cycle & 1/32" sphere packing
6000 C_1GHSV; 98.4% ΔH_C Recovery

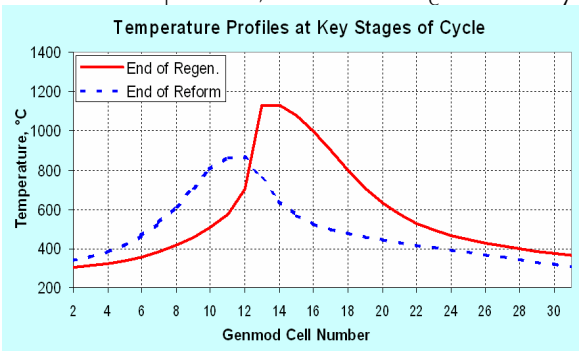

Heat Transfer Rate Requirement for High Space Velocity

The discussion above illustrates the requirement that increased space velocity be accompanied by adequate heat capacity to accommodate the reforming heat that will be required in each cycle. A second requirement is that the bed system must provide an adequate heat transfer ***rate*** to transfer this reforming heat between the bed and the gases in the time frame of the cycle. In practice, the way this rate requirement manifests itself is in the sharpness of the temperature profiles.

The primary way to increase heat transfer rate, for a fixed gases and bed type, is to increase heat transfer surface area - in essence to make the catalyst particles smaller. In Figure 3, below, the profile from Figure 2b is shown again as 3b and compared to profiles obtained using the same operation (cycle time & GHSV) but substituting larger-diameter sphere packing. It is seen that the profiles are much steeper using the 1/32" beads (3b) than using the 1/8" beads (3a). While the overall, volumetric, heat transfer coefficient depends on several geometric factors, a dominant component is the heat transfer surface area. This area is four times larger in the bed of

1/32" beads. The 1/8" bead bed would have been adequate at lower space velocity, but at 6000 C_1GHSV provides inadequate heat transfer rate. The external manifestation of the flat temperature profile is a gas exit temperature that is elevated above the inlet temperature. This significantly reduces the recovery of fuel heating value, in this example from 98% for the 1/32"beads to 94% for the 1/8" beads.

Figure 3: End-of-step temperature profiles for sphere packing using 6000 C_1GHSV and 15 second cycle. Role of heat transfer in sharpening profiles.

(a) 1/8" spheres, 93.7% ΔH_C Recovery

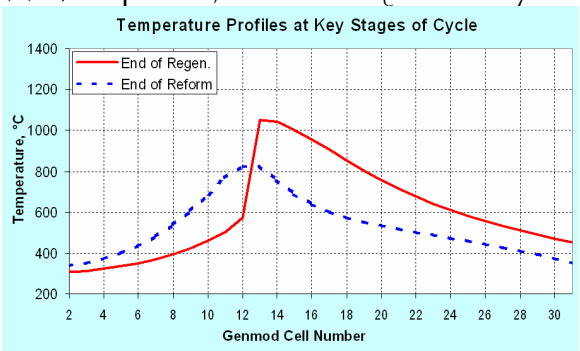

(b) 1/32" spheres, 98.4% ΔH_C Recovery

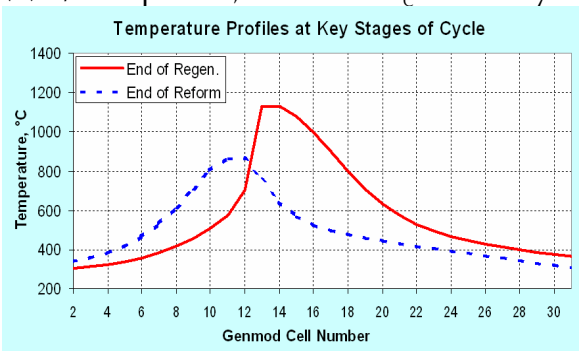

Operating Space Summary

In Figure 1, it was seen that recovery of heat value (ΔH_C) decreases with increasing space velocity (C_1GHSV) for fixed bed configuration and cycle time ($\boldsymbol{\tau}_{cycle}$). The ΔH_C-recovery can be plotted against space velocity, as shown in Figure 4(a). In this specific plot, space velocity has been translated from chemical engineering units (hr^{-1}) into practical units of how much hydrogen can be produced per liter of reactor volume. The results of the simulations of Figure 1 are shown as the yellow squares in 4(a).

Figure 4: Summary charts showing PSR operating space over range of bed packing.

(a) ΔH_C Recovery vs. Rxr Productivity

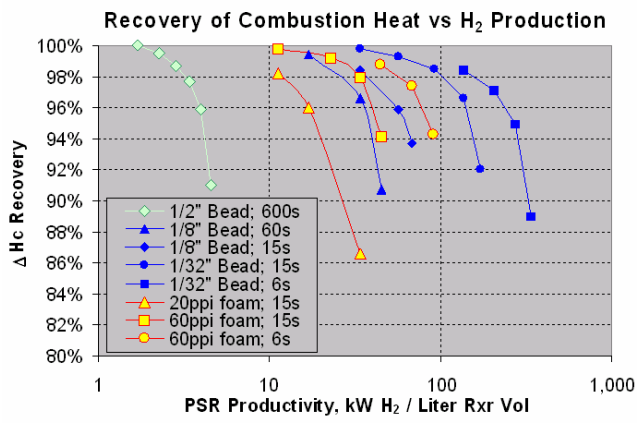

(b) Cycle Time vs. C1GHSV Map

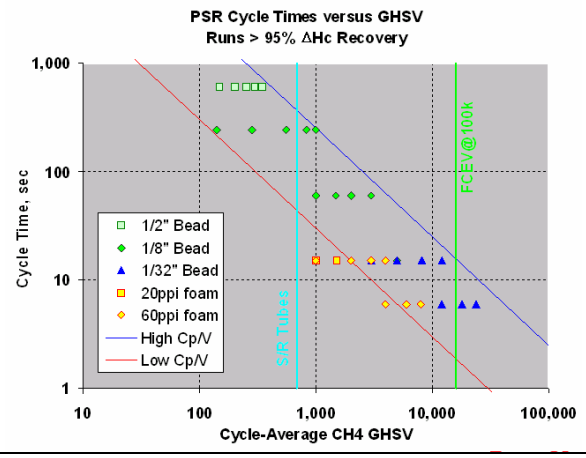

The results for many other combinations of bed packing and cycle time are also plotted on Figure 4(a). All of the parameters described so far can be seen in this chart. Finer bed packing is needed at higher productivity to increase heat transfer. Shorter τ_{cycle} enables higher productivity for a fixed-bed packing, and higher bed heat capacity (beads vs. foams) enable yet higher productivity.

A different way of looking at this information is to plot each point on a map of τ_{cycle} vs. C_1GHSV, as shown in Figure 4(b). This plot includes only higher-quality runs, defined as achieving ΔH_C recovery of greater than 95%. It is seen that the broad sweep of data follows the general rule that τ_{cycle} is inversely proportional to C_1GHSV. This inverse proportionality comes from the cyclic use of a limited amount of heat capacity. That heat can either be used slowly (low GHSV, high τ) or rapidly (high GHSV, low τ). The broad range of points within the band of inverse-proportionality comes from (a) the variability of packing heat capacity, and (b) the fact that one can always choose to operate the system at less than full utilization of the heat capacity (e.g. as in Figure 1a). In addition, it is seen that achieving higher GHSV requires transitioning to bed packing with higher volumetric heat transfer.

For reference, vertical lines are drawn in Figure 4b representing the C_1GHSV of conventional steam reforming (~700) and of air-blown catalytic autothermal reforming at a high target space velocity of 100k (in ATR units, which include air and steam). It is seen that PSR operating space extends to space velocities well above conventional steam reforming, and includes the high target space velocities desirable for compact on-board fuel reforming. While conventional 0.5 to 1.0-inch steam-reforming catalysts may be adequate at C_1GHSV of 100; new bed systems, providing higher heat transfer, are applied to achieve high space velocity.

Conclusions

When a reverse flow reactor is used to execute steam reforming, the operating space is defined by the fundamental feature that the bed itself is storing the heat of reaction from one part of the cycle to the next. A consequence of using the bed as heat reservoir is that space velocity becomes inversely proportional to cycle time for a fixed amount of heat storage. In addition, the catalyst system must be concerned with more than just kinetics and mass transfer. In this new reverse-flow reactor, providing sufficient heat transfer is the key to achieving the efficient heat exchange that is needed from the catalyst bed.

Literature

Hershkowitz, F., Berlowitz, P. J., Deckman, H. W., Marucchi-Soos, E., Gurciullo, C. S., Frederick, J. W., Rados, N., Agnihotri, R., "A Breakthrough Process for the Production of Hydrogen", AIChE Annual meeting, Fuel Cell Topical Conference paper 23D, November 2004.

Xu, J, and Froment, G. F., "Methane Steam Reforming, Methanation and Water-Gas Shift: I. Intrinsic Kinetics" AIChE Journal 35(1) 88-96 (1989).